

## Numerical determination of the phase diagram for the $\varphi^4$ model in two dimensions

Raul Toral\* and Amitabha Chakrabarti†

*Physics Department, Lehigh University, Bethlehem, Pennsylvania 18015*

(Received 26 March 1990)

By using a heat-bath Monte Carlo method, combined with extrapolation techniques developed by Ferrenberg and Swendsen [Phys. Rev. Lett. **61**, 2635 (1988)], we have determined the line of critical points in the parameter space for the  $\varphi^4$  model on a square lattice. The critical values of the parameters allow us to plot the complete phase diagram of the model. We compare the efficiency of the method to previous results based on numerical solutions of a Langevin equation. In the phase diagram we also show the locations of some of the points where numerical studies of spinodal decomposition have been carried out by several authors.

### I. INTRODUCTION

One of the most commonly used models for the study of phase transitions and critical phenomena is the  $\varphi^4$  continuum-field model.<sup>1</sup> The model is defined by a classical scalar field  $\varphi(\mathbf{r})$  whose statistical properties are governed by the Hamiltonian

$$\beta H = \int d\mathbf{r} \left[ \frac{-b}{2} \varphi^2 + \frac{u}{4} \varphi^4 + \frac{K}{2} (\nabla\varphi)^2 \right]. \quad (1.1)$$

The static critical properties of this model are generally accepted to be in the same universality class as the Ising model and to be “equivalent” to many other scalar models. This equivalence is understood in the sense that the scaling functions (when rewritten in terms of appropriate rescaled variables) and the critical exponents are the same in both models (this equivalence between the  $\varphi^4$  and the Ising model, however, has been questioned by some authors<sup>2</sup>). Although one can “derive” the  $\varphi^4$  model from the Ising model by a suitable coarse-graining procedure, this derivation is not rigorous and it is not possible to write down an exact relation between the parameters of the two models. In particular, it is believed that additional terms in the power-series expansion of the field  $\varphi$  (i.e.,  $\varphi^6$ , etc.) are required to faithfully reproduce the Ising model when far away from criticality.<sup>3</sup> Of course, it is also possible to think of the  $\varphi^4$  model as a *fundamental* model for many physical systems, without any specific reference to the Ising model. The gradient term and the  $\varphi^2, \varphi^4$  terms are then understood as the lowest-order relevant terms in an expansion of the free energy, since a renormalization-group analysis points out that higher-order terms are irrelevant to critical behavior.<sup>4</sup> It is also possible to recover (exactly) the Ising model as a particular limit of the  $\varphi^4$  model by taking the limit  $u \rightarrow \infty$  and  $b \rightarrow \infty$  such that  $b/u = \text{const}$ . This is the so-called Ising limit of the model, which should not be confused with the relation between the coarse-grained Ising model and the  $\varphi^4$  model. Since the  $\varphi^4$  model is the basis for theoretical studies of various different types of phase transitions (such as magnetic, structural, etc.), in many of these studies one is actually interested in a different limit, the so-

called displacive limit ( $u \rightarrow 0$  and  $b \rightarrow 0$ ).<sup>5</sup> Although the critical properties of the  $\varphi^4$  model have been extensively studied, the results have always been limited to general properties independent of the exact value of the parameters ( $\epsilon$  expansion) or for values of the parameters close to the Ising limit. The latter studies have been carried out by Monte Carlo,<sup>6</sup> real-space renormalization,<sup>7</sup> Migdal-Kadanoff transformation,<sup>8</sup> and molecular-dynamics methods.<sup>9</sup>

Different dynamical versions of the  $\varphi^4$  model have also been proposed depending on whether or not the order parameter is conserved.<sup>10</sup> These are generally based on stochastic differential equations of the Langevin type. Again, one could think of these dynamics as “derived” from a coarse graining of the Kawasaki dynamics or the Glauber kinetic Ising models, respectively.<sup>11</sup> This identification is very difficult to carry out quantitatively. Alternatively, one could think of the Langevin models representing the *fundamental* dynamics in some physical systems. These Langevin models (for both the conserved and nonconserved cases) have been extensively studied by analytical methods and computer simulation techniques in order to understand the ordering processes in systems quenched from an initial disordered state to deep inside the coexistence curves.<sup>12</sup> An examination of all these simulation studies indicate that the values of the parameters chosen in these different studies are closer to the displacive limit than to the Ising limit and it is interesting to study the phase diagram for these range of values for the parameters.

In this paper, we carry out numerical calculations to determine the phase diagram and the critical values for the parameters by using a new method. The method is appropriate to study the  $\varphi^4$  model for small values of the parameters  $b$  and  $u$ . We also use an extrapolation scheme derived by Ferrenberg and Swendsen<sup>13</sup> to precisely determine the maxima of quantities such as the susceptibility and specific heat.

The rest of the paper is organized as follows. In Sec. II we describe the model used by us in more detail and discuss the relation between the parametrizations used by us to those used by other authors. In Sec. III we provide the details of the numerical techniques used in this study, and

in Sec. IV we present the results obtained by using these techniques. In Sec. V we discuss the relation of the Monte Carlo study used here to the numerical integration technique used by several authors for the corresponding Langevin equations. Finally, in Sec. VI we conclude with a brief summary and conclusions.

## II. THE MODEL AND ITS RELATION TO OTHER PARAMETRIZATIONS

We consider scalar fields  $\{\Phi_i\}$   $i=1, \dots, N$ , defined on the sites  $i$  of a regular lattice in  $d$  dimensions. The spacing  $a_0$  of the lattice is considered to be unity. Periodic boundary conditions are assumed. The Hamiltonian of the model is given by

$$\beta H\{\Phi_i\} = \sum_i \left[ -\frac{b}{2}\Phi_i^2 + \frac{u}{4}\Phi_i^4 + \frac{K}{2} \sum_{\mu=1}^d (\Phi_{i_\mu} - \Phi_i)^2 \right] \quad (2.1)$$

and the equilibrium properties of this model are obtained from the partition function:

$$\begin{aligned} Z(b, u, K) &= \sum_{\{\Phi_i\}} e^{-\beta H\{\Phi_i\}} \\ &= \int_{-\infty}^{+\infty} \left[ \prod_{i=1}^N d\Phi_i \right] e^{-\beta H\{\Phi_i\}}. \end{aligned} \quad (2.2)$$

Here, as usual,  $\beta = 1/k_B T$ . The first sum in Eq. (2.1) runs over the  $N = L^d$  sites of the lattice. If  $(j_1, j_2, \dots, j_d)$  are the coordinates of site  $i$ , then the index  $i_\mu$  denotes a nearest neighbor of site  $i$  with coordinates  $(j_1, \dots, j_\mu + 1, \dots, j_d)$ .

Clearly, one of the three parameters  $b$ ,  $u$ , and  $K$  used in the model is redundant because it can be absorbed in the definition of the field variables. Many different parametrizations with only two independent parameters have been used in the literature. Although it is certainly true that each of the different parametrizations used before is useful for some particular calculation, we would like to use a very simple parametrization suitable for general purpose: we absorb a factor of  $K^{1/2}$  in the field definition and change the other parameters accordingly such that the form of the Hamiltonian remains unchanged. Specifically, we introduce a new field  $\varphi$  related to  $\Phi$  by

$$\varphi = K^{1/2} \Phi \quad (2.3)$$

and two new parameters  $\theta$  and  $\chi$  as

$$\theta = b/K \quad (2.4)$$

and

$$\chi = u/K^2 \quad (2.5)$$

so that the Hamiltonian can be written as

$$\beta H\{\varphi_i\} = \sum_i \left[ -\frac{\theta}{2}\varphi_i^2 + \frac{\chi}{4}\varphi_i^4 + \frac{1}{2} \sum_{\mu=1}^d (\varphi_{i_\mu} - \varphi_i)^2 \right]. \quad (2.6)$$

Expanding the square-term in Eq. (2.6) and using the periodic boundary conditions, this Hamiltonian can be

written as the sum of two terms:

$$\beta H\{\varphi_i\} = \beta H_0 + \beta H_I, \quad (2.7)$$

where

$$\beta H_0\{\varphi_i\} = \sum_i \left[ \left( d - \frac{\theta}{2} \right) \varphi_i^2 + \frac{\chi}{4} \varphi_i^4 \right] \quad (2.8)$$

and

$$\beta H_I\{\varphi_i\} = - \sum_{\langle ij \rangle} \varphi_i \varphi_j. \quad (2.9)$$

Here the sum in  $H_I$  runs over all the nearest-neighbors pairs of sites. Let us now identify the relation of this particular parametrization to some others used in the literature in the following paragraphs.

### A. The parametrization of Milchev, Heermann, and Binder (Ref. 6)

They consider two cases.

$$1. \quad -b + 2dK < 0$$

This is equivalent to  $\theta > 2d$ . They introduce new fields  $m_i$  and new constants  $\tilde{\alpha}$  and  $\tilde{\beta}$  as

$$\tilde{\alpha} = \frac{(-b + 2dK)^2}{u} = \frac{(-\theta + 2d)^2}{\chi}, \quad (2.10a)$$

$$\tilde{\beta} = \frac{-K(-b + 2dK)}{u} = \frac{\theta - 2d}{\chi}, \quad (2.10b)$$

$$m_i = \frac{\varphi_i}{[(b - 2dK)/u]^{1/2}} = \frac{\varphi_i}{[(\theta - 2d)/\chi]^{1/2}}. \quad (2.10c)$$

$$2. \quad -b + 2dK > 0.$$

Or,  $\theta < 2d$ . The new fields and constants are now given by

$$\tilde{\alpha} = \frac{(-b + 2dK)^2}{u} = \frac{(-\theta + 2d)^2}{\chi}, \quad (2.11a)$$

$$\tilde{\beta} = \frac{K(-b + 2dK)}{u} = \frac{-\theta + 2d}{\chi}, \quad (2.11b)$$

$$m_i = \frac{\varphi_i}{[(-b + 2dK)/u]^{1/2}} = \frac{\varphi_i}{[(-\theta + 2d)/\chi]^{1/2}}. \quad (2.11c)$$

We will be considering only the case  $\theta < 2d$ . In that case, the above relations can be inverted to obtain

$$\theta = 2d - \frac{\tilde{\alpha}}{\tilde{\beta}}, \quad (2.12a)$$

$$\chi = \frac{\tilde{\alpha}}{\tilde{\beta}^2}, \quad (2.12b)$$

$$\varphi_i = m_i \tilde{\beta}^{1/2}. \quad (2.12c)$$

### B. The parametrization of Burkhardt and Kinzel (Ref. 7)

They introduce two new parameters  $K$  and  $L$  which we will call  $K_{BK}$  and  $L_{BK}$  to avoid confusion with our notation, as

$$K_{\text{BK}} = \frac{bK}{u} = \frac{\theta}{\chi}, \quad (2.13a)$$

$$L_{\text{BK}} = \frac{b^2}{4u} = \frac{\theta^2}{4\chi}. \quad (2.13b)$$

These can be inverted as

$$\theta = \frac{4L_{\text{BW}}}{K_{\text{BW}}}, \quad (2.14a)$$

$$\chi = \frac{4L_{\text{BW}}}{K_{\text{BW}}^2}. \quad (2.14b)$$

Some other reparametrizations used in the context of phase separation studies will be discussed in Sec. V.

Since we are interested in the equilibrium properties of this model, we would like to determine the values of the parameters  $\theta$  and  $\chi$ , for which the system is in an ordered phase. In other words, we want to determine the line of critical points  $\theta_c(\chi)$ . Let us explore first all the possible values for which we expect a phase transition. First of all, if  $\chi < 0$ , the integrals appearing in the partition function are not well defined and the model has no meaning. If  $\theta < 0$  on the other hand, the local potential  $V(\varphi)$  has only one local minimum, i.e., only one ground state is stable and there cannot be a symmetry breaking. We are then led to the study of the parameter region  $0 \leq \theta \leq \infty$ ,  $0 \leq \chi \leq \infty$ . Previous studies of this problem have been concerned mostly about the Ising limit of the model for which  $\theta \rightarrow \infty$  and  $\chi \rightarrow \infty$  but  $\theta/\chi$  remains constant.

### III. NUMERICAL TECHNIQUES

Since an exact calculation of the  $N$ -dimensional integrals appearing in the partition function is impossible, we have resorted to Monte Carlo methods<sup>13</sup> for their evaluation. For this purpose, we need to generate configurations  $\{\varphi_i\}_{i=1, \dots, N}$  with a probability density function  $P_{\theta, \chi}(\{\varphi_i\})$  given by

$$P_{\theta, \chi}(\{\varphi_i\}) = e^{-\beta H\{\varphi_i\}} / Z(\theta, \chi), \quad (3.1)$$

where

$$Z(\theta, \chi) = \sum_{\{\varphi_i\}} e^{-\beta H\{\varphi_i\}} \\ = \int_{-\infty}^{+\infty} \left[ \prod_{i=1}^N d\varphi_i \right] e^{-\beta H\{\varphi_i\}}. \quad (3.2)$$

The Monte Carlo procedure consists, in general, of generating a new value for the field  $\varphi_i$  in site  $i$  using the present values of  $\varphi_i$  and its neighbors (with which it interacts). Two different methods have been used: Milchev, Heermann, and Binder<sup>6</sup> generate a new value for the field  $\varphi_i$  with a probability density function given by  $\exp(-\beta H_0)$ . This can be done exactly since  $H_0$  is a sum of terms each of which depends only on the field at site  $i$ . The interaction term  $H_I$  is then dealt with using the ordinary Metropolis algorithm. Bruce,<sup>14</sup> in his study of the "border model" ( $\theta = 2d$ ), uses a similar procedure. He approximates the probability density function for the field by the sum of two Gaussian functions. Then a standard Metropolis algorithm is executed using the difference between the real probability density function and the approximate one. Here we consider an alternate scheme. Let us consider a particular location  $i$ . The field  $\varphi_i$  in that location has a probability density function  $P_{\theta, \chi}(\varphi_i)$  given by

$$P_{\theta, \chi}(\varphi_i) = Z^{-1} \int_{-\infty}^{+\infty} \left[ \prod_{j \neq i} d\varphi_j \right] e^{-\beta H\{\varphi_j\}}. \quad (3.3)$$

In order to generate a field configuration with this probability density function, we use the heat-bath Monte Carlo method.<sup>15</sup> A new field at site  $i$  is generated with a probability density function  $\hat{P}_{\theta, \chi}(\varphi_i)$  depending on the states of the neighbors of site  $i$  as

$$\hat{P}_{\theta, \chi}(\varphi_i) = \frac{\exp \left[ -(d - \theta/2)\varphi_i^2 - \frac{\chi}{4}\varphi_i^4 + \varphi_i \sum_u \varphi_{i_u} \right]}{\int_{-\infty}^{\infty} d\varphi_i \exp \left[ -(d - \theta/2)\varphi_i^2 - \frac{\chi}{4}\varphi_i^4 + \varphi_i \sum_u \varphi_{i_u} \right]}. \quad (3.4)$$

Here the index  $i_u$  runs over the nearest neighbors of site  $i$  and  $\hat{P}_{\theta, \chi}(\varphi_i)$  is an unbiased estimator of  $P_{\theta, \chi}(\varphi_i)$ .

If we write  $a = d - \theta/2$ ,  $b = \chi/4$ , and  $c = \sum_u \varphi_{i_u}$ , Eq. (3.4) can be written as

$$\hat{P}_{\theta, \chi}(\varphi_i) = f(\varphi_i) / \int_{-\infty}^{+\infty} d\varphi_i f(\varphi_i), \quad (3.5)$$

where

$$f(\varphi_i) = f_1(\varphi_i) f_2(\varphi_i) \quad (3.6)$$

and

$$f_1(\varphi_i) = \frac{1}{(2\pi/a)^{1/2}} e^{-a(\varphi_i - c/2a)^2} \quad (3.7)$$

and

$$f_2(\varphi_i) = e^{-b\varphi_i^4}, \quad (3.8)$$

respectively. In the above calculation  $f(\varphi_i)$  is the product of a Gaussian distribution  $f_1(\varphi_i)$  and another function  $f_2(\varphi_i)$ . To sample the distribution  $f(\varphi_i)$  we generate the Gaussian part exactly by using the Box-Muller algorithm and the function  $f_2(\varphi_i)$  by a rejection technique,<sup>16</sup> i.e., we first generate a Gaussian distributed random number  $\xi$  of mean  $(c/2a)$  and variance  $\sigma = (a)^{1/2}$ . Then we generate another random number  $\eta$  uniformly distributed between 0 and 1. If  $\eta < f_2(\xi)$ , then  $\varphi_i$  takes the value  $\xi$ . Otherwise, the value  $\xi$  is rejected. We visit

the lattice in a checkerboard fashion. This method assumes that  $a$  is positive and is thus limited to values  $\theta < 2d$ . The acceptance ratio of the rejection part of the algorithm is quite large and depends on the particular values of the parameters  $\theta$  and  $\chi$ .

In order to obtain accurate estimates for the different quantities computed in the simulation we have applied the extrapolation technique introduced by Ferrenberg and Swendsen.<sup>13</sup> Let us introduce the following notation:

$$M_0 = \sum_i \varphi_i, \quad (3.9a)$$

$$M_1 = \sum_i \varphi_i^2, \quad (3.9b)$$

$$M_2 = \sum_i \varphi_i^4, \quad (3.9c)$$

$$M_3 = \sum_i \sum_{\mu=1}^d (\varphi_{i_\mu} - \varphi_i)^2. \quad (3.9d)$$

The simulation then generates configurations with a probability density function which only depends on  $M_1$ ,  $M_2$ , and  $M_3$ , namely,

$$P_{\theta,\chi}(M_1, M_2, M_3)$$

$$= \frac{N(M_1, M_2, M_3) \exp \left[ \frac{\theta}{2} M_1 - \frac{\chi}{4} M_2 - \frac{1}{2} M_3 \right]}{Z(\theta, \chi)}. \quad (3.10)$$

Here  $N(M_1, M_2, M_3)$  is such that the number of configurations with values of  $M_i$  between  $M_i$  and  $M_i + dM_i$  ( $i = 1, 2, 3$ ) is

$$N(M_1, M_2, M_3) dM_1 dM_2 dM_3.$$

Since the partition function  $Z(\theta, \chi)$  is the integral over all the possible values of  $M_1, M_2, M_3$  of the numerator of the above expression,

$$Z(\theta, \chi) = \int dM_1 dM_2 dM_3 N(M_1, M_2, M_3) \times \exp \left[ \frac{\theta}{2} M_1 - \frac{\chi}{4} M_2 - \frac{1}{2} M_3 \right], \quad (3.11)$$

the averages of any function  $f(M_i)$  of the variables  $M_i$  can be obtained as

$$\langle f(M_i) \rangle_{\theta, \chi} = \int dM_1 dM_2 dM_3 P_{\theta, \chi}(M_1, M_2, M_3) f(M_i). \quad (3.12)$$

The Ferrenberg-Swendsen extrapolation scheme allows one to compute the probability density function  $P_{\theta', \chi'}(M_i)$  if the corresponding probability  $P_{\theta, \chi}(M_i)$  is known. For our particular model, the method is based on the exact relation

$$P_{\theta', \chi'}(M_i) = \frac{P_{\theta, \chi}(M_i) \exp \left[ \frac{\theta' - \theta}{2} M_1 - \frac{\chi' - \chi}{4} M_2 \right]}{\int dM_1 dM_2 P_{\theta, \chi}(M_i) \exp \left[ \frac{\theta' - \theta}{2} M_1 - \frac{\chi' - \chi}{4} M_2 \right]} \quad (3.13)$$

between the probabilities  $P_{\theta, \chi}(M_i)$  and  $P_{\theta', \chi'}(M_i)$  for two sets of parameter values  $(\theta, \chi)$  and  $(\theta', \chi')$ . For  $\chi' = \chi$ , a case that we will be using later, the expression (3.13) simplifies to

$$P_{\theta', \chi}(M_i) = \frac{P_{\theta, \chi}(M_i) \exp \left[ \frac{\theta' - \theta}{2} M_i \right]}{\int dM_i P_{\theta, \chi}(M_i) \exp \left[ \frac{\theta' - \theta}{2} M_i \right]}. \quad (3.14)$$

In practice, this extrapolation scheme fails to work if the value  $\theta'$  is much different from that of  $\theta$ . In that case, the information gathered in  $P_{\theta, \chi}(M_i)$  in a numerical calculation is not enough to yield a precise determination of  $P_{\theta', \chi'}(M_i)$ . We have used the following criterion to decide which extrapolation range we should allow. We compute the standard deviation of  $M_1$ ,  $\sigma(M_1)$ , and allow a variation  $\Delta\theta$  such that the relation  $\Delta\theta\sigma(M_1)/2 < 1$  is satisfied. That ensures that the exponentials appearing in (3.14) do not take any large values. We have found that  $\Delta\theta$  increases when  $\theta$  approaches the critical value  $\theta_c$  and that  $\Delta\theta$  decreases with increasing  $L$  as  $\Delta\theta \sim L^{-1/\nu}$  as predicted.<sup>16,17</sup>

#### IV. RESULTS

For a given value of the parameters  $\theta$  and  $\chi$  we have generated  $N_m$  field configurations by using the method described in the previous section. To increase the statistical independence of the configurations, we have updated the system for  $N_u$  lattice updates before a field configuration is incorporated into the statistics. We started by setting all the field values in every lattice site equal to the mean-field equilibrium value  $\varphi_{MF} = (\theta/\chi)^{1/2}$ .  $N_0$  lattice updates are then executed in order to thermalize the lattice. The particular values of  $N_0$ ,  $N_m$ , and  $N_u$  depend on the lattice size  $L$ . The values of  $L$  considered are  $L = 8, 16, 24, 32$ , and  $40$ . The simulation details are summarized in Table I.

We have considered values of  $\chi = 1, 0.7, 0.5, 0.25, 0.1$ , and  $0.05$ . For every value of  $\chi$  we have generated independent equilibrium configurations corresponding to several values of  $\theta$ . Typically, we would make some short trial runs to determine the ‘‘interesting’’ range of values for  $\theta$ . This would correspond to those values of  $\theta$  such that well-defined maxima appear in the specific heat and the susceptibility. Once the range of values of  $\theta$  has been approximately determined, two long runs were carried out with the parameters of Table I such that, by extrapolating according to the method explained in the previous sections, we obtained information about a large enough

TABLE I. Simulation details.

$L$	$N_0$	$N_u$	$N_m$
8	$10^4$	1	$10^6$
16	$5 \times 10^4$	5	$10^6$
24	$10^5$	5	$5 \times 10^5$
32	$10^5$	10	$10^5$
40	$10^5$	10	$10^5$

interval for the parameter  $\theta$ .

We have computed, among other quantities, the values of  $M_0$ ,  $M_1$ ,  $M_2$ , and  $M_3$  during the simulation as a function of  $\theta$  and  $\chi$ . Other quantities of interest are, for instance, the total magnetization  $M$ ,

$$M = \langle |M_0| \rangle, \quad (4.1)$$

the total energy  $E$ ,

$$E = \left\langle -\frac{\theta}{2}M_1 + \frac{\chi}{4}M_2 + \frac{1}{2}M_3 \right\rangle, \quad (4.2)$$

and the corresponding intensive magnitudes  $e = E/N$ ,  $m = M/N$ . Figure 1 shows the magnetization  $m$  as a function of  $\theta$  in the case of  $\chi=1$ . We stress here that Fig. 1 (as well as many of the other figures in this paper) has been generated by carrying out simulations just at two different values of  $\theta$  for every value of  $L$ . The values of  $m$  at other values of  $\theta$  are found by using the extrapolation method described above, allowing us to obtain smooth and essentially continuous curves for  $m$  versus  $\theta$ . The fact that the extrapolated values obtained from the two selected values of  $\theta$  agree within the statistical errors gives further support to the validity of the extrapolation scheme for this model. Figure 2 is a plot of the energy  $e$  as a function of  $\theta$  with  $\chi=0.1$ . Again, the extrapolation provides smooth continuous curves.

The fluctuations in the energy and the magnetization

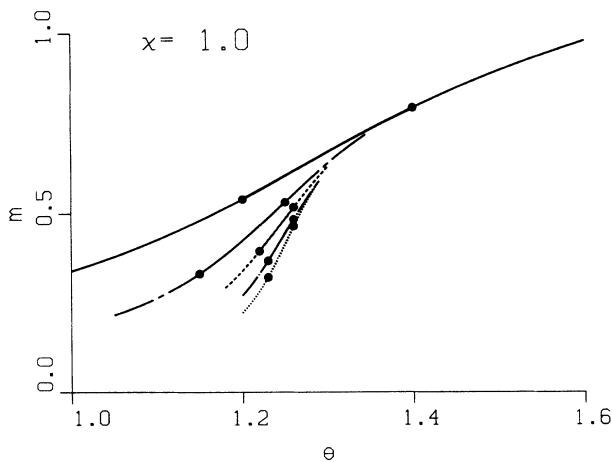


FIG. 1. Spontaneous magnetization  $m$  as a function of  $\theta$  for  $\chi=1$  and for different values for  $L$  as follows:  $L=8$  (—),  $L=16$  (---),  $L=24$  (···),  $L=32$  (-·-·-),  $L=40$  (- - - -). For each value of  $L$  the whole curve has been obtained by extrapolation from data coming from two simulations at two different values for  $\theta$ . These  $\theta$  values are indicated by circles on the curves.

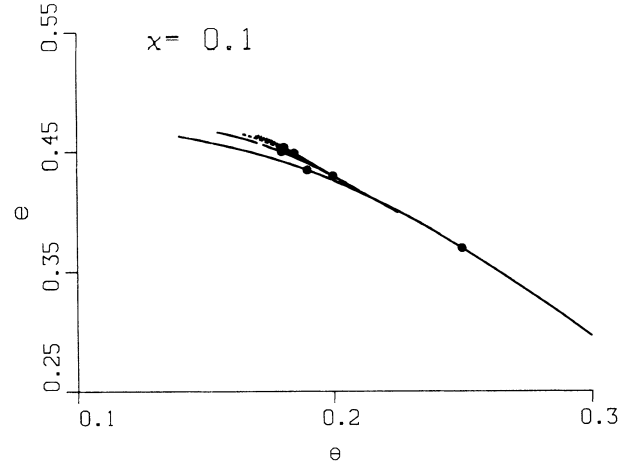


FIG. 2. Energy  $e$  as a function of  $\theta$  for  $\chi=0.1$ . Same line types and symbols as in Fig. 1.

allows one to compute the specific heat  $C$  and the susceptibility  $\kappa$ , respectively, as (irrelevant constants are dropped out)

$$C = (\langle E^2 \rangle - \langle E \rangle^2) / N \quad (4.3)$$

and

$$\kappa = (\langle M^2 \rangle - \langle M \rangle^2) / N. \quad (4.4)$$

Figure 3 shows a plot of the specific heat  $C$  as a function of  $\theta$  for  $\chi=1$ . Figure 4 plots the susceptibility  $\kappa$  versus  $\theta$  for  $\chi=0.1$ . Note that in both figures there are well-defined maxima whose location can be very precisely determined. At the critical value  $\theta_c(\chi)$ ,  $C$  and  $\kappa$  would develop singularities of the type  $C \sim |\theta - \theta_c|^{-\alpha}$  (or  $C \sim \ln|\theta - \theta_c|$  in two dimensions),  $\kappa \sim |\theta - \theta_c|^{-\gamma}$ , with  $\alpha$  and  $\gamma$  the usual critical exponents. Strictly speaking, these singularities only appear in an infinite system. For a finite system containing  $N=L^d$  sites,  $C$  and  $\kappa$  have maxima at locations  $\theta_c^1(L)$  and  $\theta_c^2(L)$ , respectively. These maxima sharpen and their location shifts with increasing  $L$  towards the asymptotic value

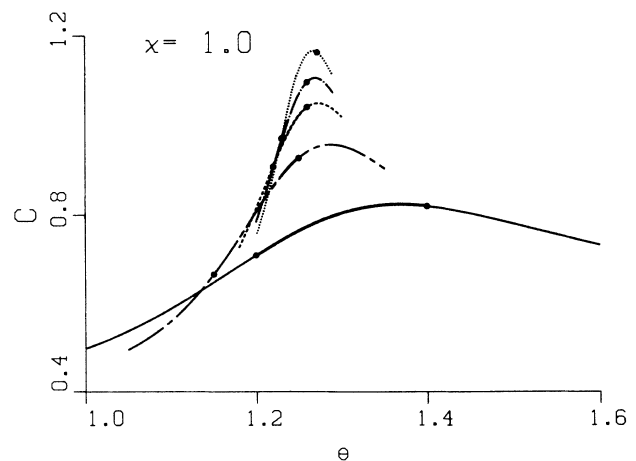


FIG. 3. Specific heat  $C$  as a function of  $\theta$  for  $\chi=1$ . Same line types and symbols as in Fig. 1.

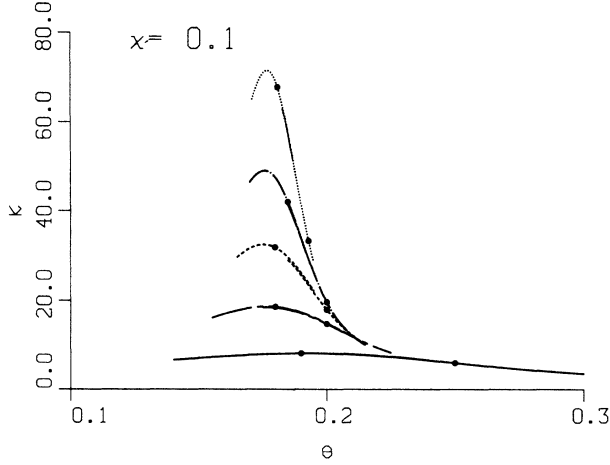


FIG. 4. Susceptibility as a function of  $\theta$  for  $\chi=0.1$ . Same line types and symbols as in Fig. 1.

$$\theta_c = \theta_c^1(L = \infty) = \theta_c^2(L = \infty).$$

Finite-size scaling theory<sup>18</sup> provides one way in which the infinite limit can be recovered. In particular, it tells us how  $\theta_c^i(L)$  should tend to  $\theta_c$ , i.e.,

$$\theta_c^i(L) = \theta_c + a_i L^{-1/\nu} + b_i L^{-\omega} + \dots, \quad i=1,2. \quad (4.5)$$

Here  $a_i$  and  $b_i$  are constants and  $\nu$  is the critical exponent characterizing the critical behavior of the correlation length ( $\nu=1$  in  $d=2$ ). As discussed before, the simulations allow us to obtain very precise values for the location of the maxima  $\theta_c^i(L)$ . In order to determine  $\theta_c$  we have to fit the  $\theta_c^i(L)$  to the expression (4.5) above. In practice, however, the fitting is not free of problems. We note that expression (4.5) is actually the beginning of an infinite series of terms incorporating all the corrections to the leading scaling behavior given by the first two terms in the right-hand side. Interpreted in this fashion one can identify  $\omega = \frac{4}{3}$  in two dimensions.<sup>19</sup> However, as we move towards the displacive limit (as  $\chi$  goes to 0), the exponent  $\nu$  in the leading term ( $a_i L^{-1/\nu}$ ) is expected to jump to the mean-field value ( $\nu = \frac{1}{2}$ ), since the transition has a mean-field character in this limit. Also, it is not clear at all which are the higher-order correction terms in Eq. (3.5) nor what their relative numerical importance is when analyzing Monte Carlo data. With these problems in mind, we have considered several methods to precisely determine the value of the critical parameter  $\theta_c$  as a function of  $\chi$ . These methods are described below.

(a) We have plotted  $\theta_c^i(L)$  versus  $1/L$  and allowed an extrapolation towards the origin by fitting the last few points in the corresponding curves by a straight line. This is shown in Figs. 5(a) and 5(b) for  $\chi=1$  and 0.1, respectively.

(b) We have considered Eq. (4.5) with  $\omega$  being a phenomenological parameter whose effective value takes into account approximately all the other correction to scaling terms. Since in the displacive limit  $\nu$  takes the mean-field value of  $\frac{1}{2}$ , we have considered that  $\omega$  can vary between 1 and 2. We have then fitted Eq. (3.5) with three adjustable

parameters ( $\theta_c$ ,  $a_i$ , and  $b_i$ ) to the simulation data, both for the specific heat ( $i=1$ ) and the susceptibility ( $i=2$ ) data. The resulting values for  $\theta_c$  agree with the ones obtained from the graphical extrapolation in Fig. 5. The dispersy of the fitted values  $\theta_c$  as  $\omega$  varies allows us to give error bars to  $\theta_c$ .

(c) In order to give further support for the assigned values of  $\theta_c$  and also to gain some insight into the importance of the correction to scaling terms, we have analyzed the scaling behavior for several quantities. Such a scaling behavior for the magnetization  $m$  is expected to be given by<sup>18</sup>

$$m(\theta, L) = L^{-\beta/\nu} f(\epsilon L^{-1/\nu}), \quad (4.6)$$

where  $\epsilon = 1 - \theta/\theta_c$ . Figure 6 shows scaling plots of the magnetization for  $\chi=1$  [Fig. 6(a)] and  $\chi=0.1$  [Fig. 6(b)]. We see that although the scaling relation (4.6) is reasonable well satisfied in both cases, the quality of the scaling is better for  $\chi=1$  than for  $\chi=0.1$  and as  $\chi$  decreases one

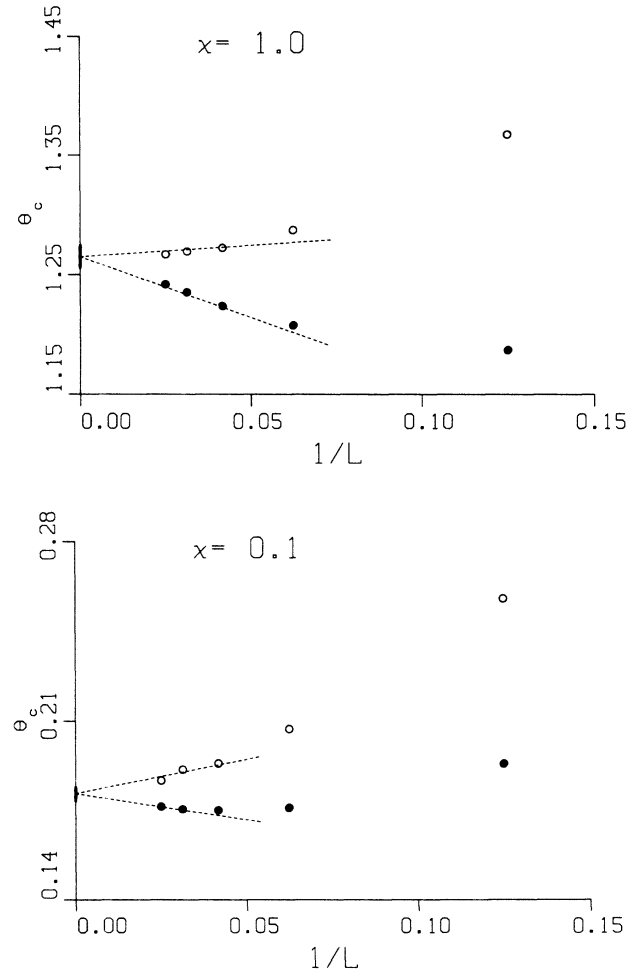


FIG. 5. (a) Plot of the pseudocritical values of  $\theta$ :  $\theta_c^1(L)$  ( $\circ$ ) and  $\theta_c^2(L)$  ( $\bullet$ ), defined as the location of the maximum of the specific heat and the susceptibility, respectively, for  $\chi=1$ . The extrapolation to the origin gives the values of the critical coupling  $\theta_c = 1.265 \pm 0.005$ . (b) Same as (a) for  $\chi=0.1$ . The calculated value for  $\theta_c$  is  $\theta_c = 0.182 \pm 0.003$ .

needs larger values of  $L$  in order to satisfy scaling. This is so because as  $\chi$  decreases towards 0 (the displacive limit) the exponents should jump to their mean-field values. This effect can be taken into account approximately<sup>6</sup> by considering some effective values for the exponents  $\nu$  and  $\beta$ . We have not pursued this approach here though, since our main goal is the determination of the critical coupling  $\theta_c(\chi)$ . We also analyze the scaling behavior of the fourth-order cumulant of the magnetization,  $\rho$ , defined as

$$\rho = 1 - \frac{\langle M^4 \rangle}{3\langle M^2 \rangle^2}. \quad (4.7)$$

(This quantity has been used previously to determine the critical coupling for several models.<sup>6,20</sup>) The scaling behavior of  $\rho$  is expected to be

$$\rho(\theta, L) = f(\epsilon L^{-1/\nu}). \quad (4.8)$$

Figures 7(a) and 7(b) show the scaling plot of the cumulant  $\rho$  for  $\chi=1$  and 0.1, respectively. The scaling relation (4.8) is satisfied for large enough values of  $L$  in both cases. For  $\chi=1$ , scaling holds for  $L \geq 16$  whereas the quality of

the scaling decreases for  $\chi=0.1$  and scaling holds only for  $L \geq 24$ .

## V. COMPARISON AND RELATION TO LANGEVIN-TYPE DYNAMICS

As mentioned earlier, it is possible to associate a dynamics to the field variables  $\{\Phi_i\}$  by using a stochastic differential equation of Langevin type

$$\frac{\partial \Phi_i}{\partial t} = -\Gamma \frac{\delta H}{\delta \Phi_i} + \eta_i(t), \quad (5.1)$$

where  $\eta_i(t)$  is a Gaussian stochastic variable of mean zero (the "noise" term). If  $\Gamma$  is simply a number, this equation represents a nonconserved field, i.e., the order parameter  $N^{-1} \sum_i \phi_i(t)$  changes with time (this corresponds to the model *A* in the taxonomy of Hohenberg and Halperin<sup>10</sup>). If, on the other hand,  $\Gamma = -M \nabla^2$ , where  $M$  is a constant and  $\nabla^2$  is the Laplacian operator, then the order parameter is conserved which corresponds to the model *B* of Hohenberg and Halperin. In both

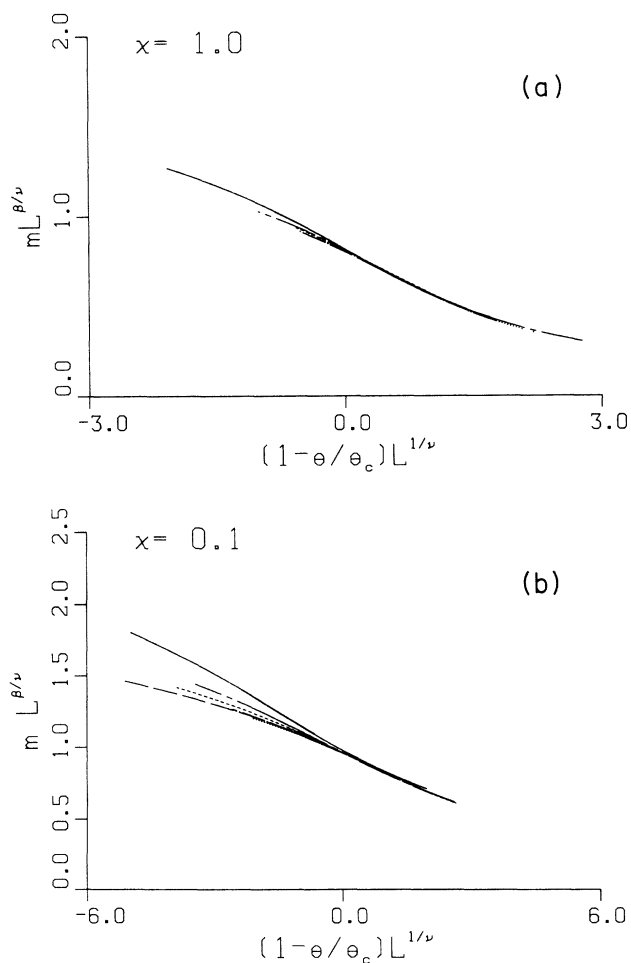


FIG. 6. (a) Plot to check the finite-size scaling behavior of the magnetization  $m$  with respect to the variables  $L$  and  $\theta$  in the case of  $\chi=1$ . The line types have the same meaning as in Fig. 1. (b) Same as (a) for  $\chi=0.1$ .

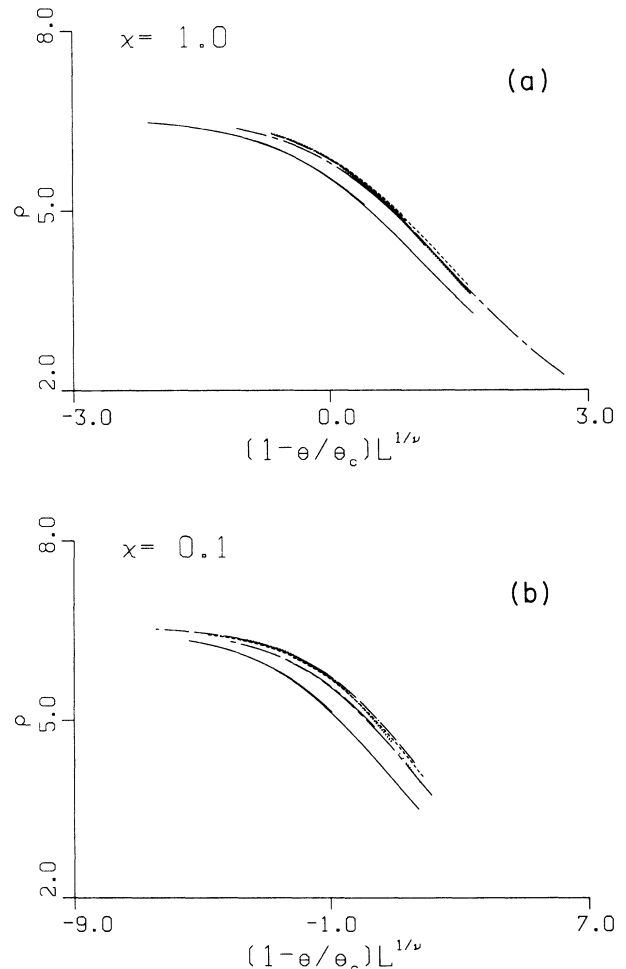


FIG. 7. (a) Plot to check the finite-size scaling behavior of the fourth-order cumulant of the magnetization  $m$  with respect to the variables  $L$  and  $\theta$  in the case  $\chi=1$ . The line types have the same meaning as in Fig. 1. (b) Same as (a) for  $\chi=0.1$ .

models  $A$  and  $B$  it is assumed that the stationary ( $t \rightarrow \infty$ ) solution of the stochastic equation corresponds to an equilibrium Gibbs distribution at temperature  $T$ . This is achieved by imposing the following constraint on the spatiotemporal correlations of the noise variable:

$$\langle \eta_i(t) \eta_j(t') \rangle = 2k_B T \Gamma \delta_{ij} \delta(t-t') \quad (5.2)$$

(the so-called fluctuation-dissipation relation). The dynamical properties of models  $A$  and  $B$  have been extensively studied analytically and numerically.<sup>12</sup> Here we are concerned with the use of the Langevin equation as a means of generating *equilibrium configurations* and determining the line of critical points, the phase diagram, and other equilibrium properties of the model. A preliminary step in that direction was carried out by Valls and Mazenko<sup>21</sup> (will be referred to as VM). They solved Eq. (5.1) numerically for model  $A$  by using a simple Euler scheme of integration. When one substitutes Eq. (2.1) for the Hamiltonian into Eq. (5.1) one obtains

$$\frac{\partial \Phi_i}{\partial t} = -k_B T \Gamma (-b \Phi_i + u \Phi_i^3 - K \nabla_i^2 \Phi_i) + \eta_i, \quad (5.3)$$

where the lattice Laplacian operator  $\nabla_i^2$  is defined by

$$\nabla_i^2 \Phi_i = \sum_u (\Phi_{i_u} - \Phi_i) \quad (5.4)$$

and the index  $i_u$  runs over the nearest neighbors of site  $i$ . We can rewrite this equation in terms of the parameters introduced in Sec. II as

$$\frac{\partial \varphi_i}{\partial t} = -\Gamma_0 (-\theta \varphi_i + \chi \varphi_i^3 - \nabla_i^2 \varphi_i) + \zeta_i, \quad (5.5)$$

where  $\Gamma_0 = k_B T K \Gamma$ , and the new noise variable  $\zeta$  satisfies

$$\langle \zeta_i(t) \zeta_j(t') \rangle = 2\Gamma_0 \delta_{ij} \delta(t-t'). \quad (5.6)$$

VM, however, use a different parametrization. They introduce two new parameters, one of which is the parameter  $\theta$  defined before and the other one is  $K_{VM}$  (just  $K$  in their notation) defined by

$$K_{VM} = K^2(1+\theta)/u = (1+\theta)/\chi, \quad (5.7)$$

the inverse relation being

$$\chi = (1+\theta)/K_{VM}. \quad (5.8)$$

In their numerical study, VM monitored the evolution of the time-dependent susceptibility  $\kappa(t)$ , defined as

$$\kappa(t) = \left\langle \frac{1}{N} \sum_{i,j} \varphi_i(t) \varphi_j(t) \right\rangle. \quad (5.9)$$

As  $\kappa(t)$  saturates at its equilibrium for large enough times, VM give the following criterion to decide whether the system is ordered or disordered: if  $\kappa(t)$  saturates at a value which is independent of  $N$  for large  $N$ , then the system is in the disordered state; if, on the other hand, the saturation value of  $\kappa(t)$  is proportional to  $N$ , then the system is ordered. This criterion allow VM to approximately determine the line of critical points. We believe, however, that the method of integrating the Langevin equation is not suitable for studying *equilibrium properties* of

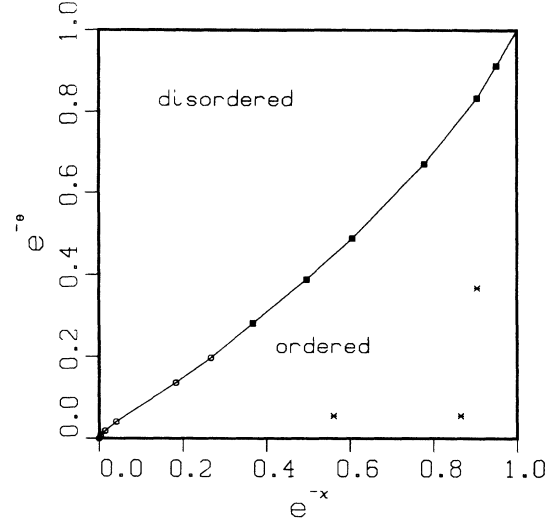


FIG. 8. Phase diagram for the model discussed in the paper (see Table II). Open circles correspond to results previously obtained by other authors (Refs. 6, 7, and 14), solid squares are the results of the present calculation. The stars are the locations where some of the numerical simulations in Ref. 23 were carried out.

the model. This is so because special care has to be taken for the choice of the time step  $\delta t$  required for the numerical integration. To make a direct comparison between the two methods we have considered a system of size  $N=18^2$  and values for the parameters  $\theta=2$ ,  $\chi=1$ . According to Fig. 8, this corresponds to a system in an ordered state (these values for the parameters were chosen because they are representative of the ones used in studies of spinodal decomposition, see below). We numerically integrated the Langevin Eq. (4.5) over a long time and made sure that the system had reached equilibrium (since we started with an initial condition for the field equal to the mean-field equilibrium value everywhere, the convergence to equilibrium is actually very fast for the parameters considered here). Once in equilibrium, we continue integrating the equation and measure the spontaneous magnetization  $m$ . We find that  $m$  depends on the time step used for the numerical integration<sup>22</sup> and that, even for  $\delta t=0.001$ , complete convergence is yet to be reached. The available data, however, allows us to extrapolate towards  $\delta t=0$  as shown in Fig. 9. The extrapolated value is in perfect agreement with the value we obtain by gen-

TABLE II. Critical value of the parameter  $\theta$  for different values of the parameter  $\chi$ , obtained in the present simulations. The numbers in parentheses indicate the uncertainty in the last digit of  $\theta_c(\chi)$ .

$\chi$	$\theta_c(\chi)$
1.0	1.265(5)
0.7	0.945(5)
0.5	0.716(4)
0.25	0.400(4)
0.1	0.182(3)
0.05	0.0905(3)

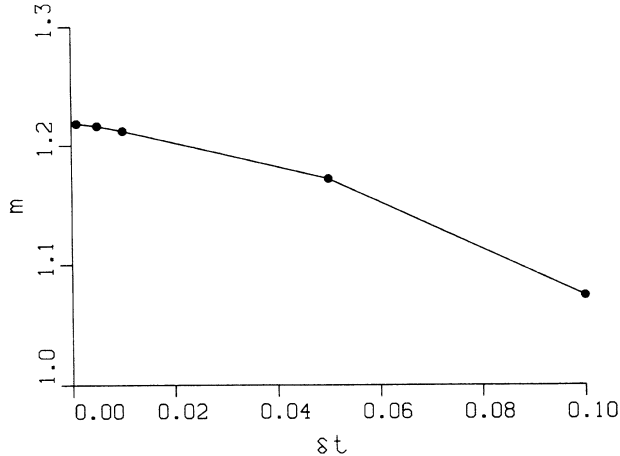


FIG. 9. Dependence of the equilibrium magnetization on the time step  $\delta t$  used to numerically solve the Langevin Eq. (4.5) for  $\theta=2$ ,  $\chi=1$ . The straight line extrapolation towards the origin gives  $m=1.220$ .

erating equilibrium configurations by the heat-bath method.

In many studies of phase separation (model *B*) in two<sup>23</sup> and three<sup>24</sup> dimensions yet another parametrization is used. This parametrization is a little confusing since it seems to imply that only one parameter (instead of two:  $\theta$  and  $\chi$ ) is necessary to describe the properties of the system. In this particular parametrization<sup>25</sup> one considered Eq. (4.1) (with  $\Gamma=M\nabla^2$ ), defined on a continuum space of vectors  $r$ , and makes the following rescalings:

$$\psi = \frac{\Phi}{(b/u)^{1/2}}, \quad (5.10a)$$

$$\tau = t \frac{Mb^2}{2k_B TK}, \quad (5.10b)$$

$$x = \frac{r}{(K/b)^{1/2}}. \quad (5.10c)$$

In terms of the rescaled variables  $\psi$ ,  $\tau$ , and  $x$ , the equation simply reads

$$\frac{\partial \psi}{\partial \tau} = \frac{1}{2} \nabla^2 (-\psi + \psi^3 - \nabla^2 \psi) + \sqrt{\epsilon} \xi, \quad (5.11)$$

where the noise variable  $\xi$  satisfies

$$\langle \xi(\mathbf{x}, t) \xi(\mathbf{x}', t') \rangle = -\nabla^2 \delta(\mathbf{x} - \mathbf{x}') \delta(t - t') \quad (5.12)$$

and the parameter  $\epsilon$  is given by

$$\epsilon = \frac{ub^{d/2-2}}{K^{d/2}} = \chi \theta^{d/2-2}. \quad (5.13)$$

Equations (5.11) and (5.12) contain only one parameter and seem to imply that systems with different  $\theta$  and  $\chi$  should have the same properties if  $\epsilon$  is kept constant. This contradiction is resolved by noticing that Eq. (5.11) and (5.12) are defined on a continuum space for the vectors  $x$  instead of a lattice as the model used in previous sections. However, the numerical solution of Eqs. (5.11) and (5.12) is achieved by replacing the Laplacian opera-

tor by a discretized (i.e., lattice defined) operator as

$$\nabla^2 \psi(x) \rightarrow (\Delta x)^{-2} \nabla_l^2 \psi_i = (\Delta x)^{-2} \sum_u (\psi_{i_u} - \psi_i). \quad (5.14)$$

We see that when (5.14) is inserted in Eq. (5.11) the resulting equation is equivalent to the lattice Eq. (5.3) with a *different* constant  $K$ , i.e.,  $K \rightarrow K/(\Delta x)^2$ . By comparing the different terms in the lattice Eq. (5.3) and the discretized version of the continuum equation (with a normalized coupling  $K$ ) it is possible to make a direct comparison between the parameters of both models. The relation is

$$\theta = (\Delta x)^2, \quad (5.15a)$$

$$\chi = \epsilon (\Delta x)^{4-d}. \quad (5.15b)$$

Available simulations of the two-dimensional Langevin equation typically<sup>23</sup> use values of  $\Delta x$  around 1 and small ( $\sim 0.1$ ) values for  $\epsilon$ . We have plotted in Fig. 8 the location of some of these simulations to show that they fall closer to the displacive limit than to the Ising limit. It is clear, then, that the methods developed in this paper can be used to determine equilibrium properties relevant in those studies of phase separation.

## VI. CONCLUSIONS

We have studied the  $\varphi^4$  model defined on a square lattice and, by using the heat-bath Monte Carlo algorithm (implemented with a rejection technique), we have generated equilibrium configurations of the model. Ensemble averages over these equilibrium configurations are combined with an extrapolation technique. This allows us to generate essentially continuous curves for the measured magnitudes of interest: energy, magnetization, specific heat, susceptibility, and others. The method is particularly useful in the vicinity of the critical region. By studying the finite-size scaling behavior of the specific heat and the susceptibility, we have been able to determine some values belonging to the line of critical points in the parameter space that separate ordered from disordered phases, thus effectively mapping out the phase diagram of the model. The method used in this paper can be used if the parameter  $\theta$  satisfies  $\theta < 2d$ , i.e., for systems between the so-called border model ( $\theta=2d$ ) and the displacive limit ( $\theta=0$ ). This range of parameters is shown to be the relevant one for some previous studies of spinodal decomposition. Further studies will include three-dimensional systems and spin glasses.

## ACKNOWLEDGMENTS

This work was supported by the National Science Foundation (NSF) Grant No. DMR-8612609 in Lehigh University. R.T. acknowledges financial support from DGICYT Project No. PB-86-0534 (Spain). Computations were carried out using the Cornell National Supercomputer Facility, a resource of the Cornell Theory Center, which is funded in part by the National Science Foundation, New York State, the IBM Corporation, and the members of the Center's Corporate Research Institute.

- \*Permanent address: Department de Fisica, Universitat de les Illes Balears, 07071-Palma de Mallorca, Spain.
- †Permanent address: Department of Physics, Kansas State University, Manhattan, KS 66506.
- <sup>1</sup>General references and properties of the  $\varphi^4$  model are exposed in D. Amit, *Field Theory, the Renormalization Group, and Critical Phenomena*, 2nd ed. (World-Scientific, Singapore 1984).
- <sup>2</sup>G. Baker and J. Johnson, *Phys. Rev. Lett.* **54**, 2461 (1985); *J. Phys. A* **17**, L275 (1984).
- <sup>3</sup>K. Kaski, K. Binder, and J. Gunton, *J. Phys. A* **16**, L623 (1983); *Phys. Rev. B* **29**, 3996 (1984).
- <sup>4</sup>K. G. Wilson and J. Kogut, *Phys. Rep. C* **12**, 77 (1974).
- <sup>5</sup>R. Cowley, *Adv. Phys.* **29**, 1 (1980); A. Bruce, *ibid.* **29**, 111 (1980); A. Bruce and R. Cowley, *ibid.* **29**, 219 (1980).
- <sup>6</sup>A. Milchev, D. Heermann, and K. Binder, *J. Stat. Phys.* **44**, 749 (1986).
- <sup>7</sup>T. Burkhardt and W. Kinzel, *Phys. Rev. B* **20**, 4730 (1979).
- <sup>8</sup>P. Beale, S. Sarker, and J. Krumhansl, *Phys. Rev. B* **24**, 266 (1981).
- <sup>9</sup>T. Schneider and E. Stoll, *Phys. Rev. B* **13**, 1216 (1976); *Phys. Rev. Lett.* **31**, 1254 (1973).
- <sup>10</sup>P. Hohenberg and B. I. Halperin, *Rev. Mod. Phys.* **49**, 435 (1977).
- <sup>11</sup>J. S. Langer, *Ann. Phys. (N.Y.)* **65**, 53 (1971); *Physica* **73**, 61 (1974).
- <sup>12</sup>A review of the field is given by J. D. Gunton, M. San Miguel, and P. Sahni, in *Phase Transitions and Critical Phenomena*, edited by C. Domb and J. L. Lebowitz (Academic, New York, 1983), Vol. 8. More recent reviews focusing on numerical results are given in J. D. Gunton *et al.*, *J. Appl. Cryst.* **21**, 811 (1988), J. D. Gunton *et al.*, *Phys. Scr.* (to be published).
- <sup>13</sup>*Monte Carlo Methods in Statistical Physics*, edited by K. Binder (Springer, Berlin, 1979); *Applications of the Monte Carlo Methods in Statistical Physics*, edited by K. Binder (Springer, Berlin, 1984).
- <sup>14</sup>A. Bruce, *J. Phys. A* **18**, L873 (1985).
- <sup>15</sup>M. Kalos and P. Whitlock, *Monte Carlo Methods, Volume I: Basics* (Wiley, New York, 1986).
- <sup>16</sup>A. Ferrenberg and R. Swendsen, *Phys. Rev. Lett.* **61**, 2635 (1988).
- <sup>17</sup>A. Ferrenberg and R. Swendsen, *Phys. Rev. Lett.* **63**, 1195 (1989).
- <sup>18</sup>For a review, see M. Barber, in *Phase Transitions and Critical Phenomena*, edited by C. Domb and J. Lebowitz (Academic, New York, 1983), Vol. 8.
- <sup>19</sup>B. Nienhuis, *J. Phys. A* **15**, 199 (1982).
- <sup>20</sup>K. Binder, *Z. Phys. B* **43**, 119 (1981).
- <sup>21</sup>O. T. Valls and G. F. Mazenko, *Phys. Rev. B* **34**, 7941 (1986).
- <sup>22</sup>A. Greiner, W. Strittmatter, and J. Honerkamp, *J. Stat. Phys.* **51**, 95 (1988).
- <sup>23</sup>E. Gawlinski, J. Vinals, and J. Gunton, *Phys. Rev. B* **39**, 7266 (1989); T. M. Rogers, K. R. Elder, and R. C. Desai, *ibid.* **37**, 9638 (1988); R. Toral, A. Chakrabarti, and J. D. Gunton, *ibid.* **39**, 901 (1989).
- <sup>24</sup>A. Chakrabarti, R. Toral, and J. D. Gunton, *Phys. Rev. B* **39**, 4386 (1989); R. Toral, A. Chakrabarti, and J. D. Gunton, *Phys. Rev. Lett.* **60**, 2311 (1988).
- <sup>25</sup>M. Grant, M. San Miguel, J. Vinals, and J. Gunton, *Phys. Rev. B* **31**, 3027 (1985).